Dynamics of the KOPIO Decays

B. Field*
C.N. Yang Institute for Theoretical Physics, Stony Brook University, Stony Brook, New York 11794-3840, USA and Department of Physics, Brookhaven National Laboratory, Upton, New York 11973-5000, USA
(Dated: August 23, 2004)

Kinematic distributions for K_L^0 decays in the KOPIO Monte Carlo (MC) are compared to analytic curves of the same quantities. New decay modes were added to the MC and compared to known distributions. Overall, the agreement was found to be excellent with no errors to report.

PACS numbers: 11.30.Er, 11.80.Cr, 12.15.Hh, 12.15.Ji, 13.25.Es

I. INTRODUCTION

Properly understanding the kinematic distributions, in this case the Dalitz plots, of K_L^0 decays is essential to detecting the signal channel in the KOPIO experiment. The Dalitz plot is a very useful tool in understanding the dynamics of different decay modes. In particular, a theoretical Dalitz distribution shows the preferred decay orientation. Although this can be done in any Lorentz frame, it is most convenient and useful to use the rest frame of the decaying particle to simplify the calculation of the matrix elements. Experimentally, bands in a measured Dalitz distribution may show other unstable particles in the decay chain before the final decay products are created. Historically this lead to the discovery of new particles. There are several excellent references for understanding Dalitz distributions. A nice overview is presented in Ref. [1].

Consider the three body decay in Fig. 1. In this decay, we can write down two experimentally accessible (and Lorentz invariant) variables, the effective masses of two pairs of the final state particles. Once the matrix elements are completed, they can be binned in any manner desired by the MC code. However, the use of Lorentz invariants make the calculation more tenable and the experimental analysis more illuminating. The two variables can be plotted and tell us about the decay in a physical way. Some of what can be deduced is shown in Fig. 2. This is particularly helpful when little if anything is known about the matrix elements themselves, as in totally hadronic processes.

However, using the invariant masses is not the only way to create a Dalitz plot. Another method is to use reduced energies. This is particularly useful in the rest frame of the decaying particle, where the matrix elements take their simplest form. The four vector of the decaying particle becomes $P = (M, \vec{0})$, so dot products with this four vector become proportional to ME_i, where the index i labels a daughter particle. In this representation, two of the final state particles are chosen, and twice their energy divided by the mass scale of the matrix elements are used as the variables. In this note, we have generically chosen these variables as follows

$$y = \frac{2E_1}{M}, \qquad z = \frac{2E_2}{M}. \tag{1}$$

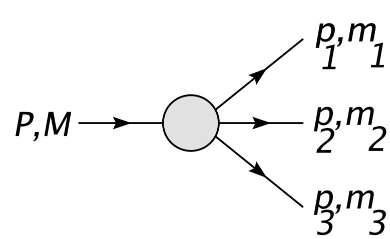

FIG. 1: A generic three body decay. The three final state particles can be broken into two sets of two, each with one common particle, usually taken to be the second particle. The standard Dalitz variables are the effective masses of those particle sets. It should be noted that Dalitz plots can in fact be constructed with realistically unobservable variables, such as the invariant mass of a neutrino pair (like in the signal channel). However, this will be ignored in this analysis.

*bfield@ic.sunysb.edu

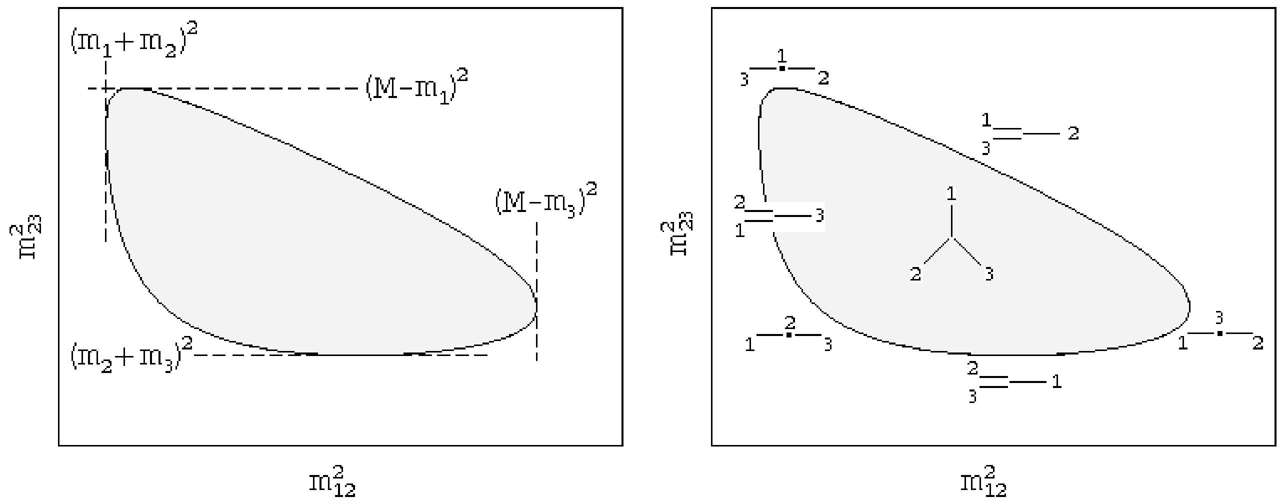

(a)

(b)

FIG. 2: Figure 2a shows how the borders of a Dalitz distribution are defined by the mass of the decaying particle M and the masses of the final state particles m_i. It it easy to see that the shape of the distribution has information about the process encoded in it. Figure 2b shows the orientation of the particles as they would populate the Dalitz distribution. When the distribution is viewed as a surface, this information can be considered as the preferred decay orientation or as the distribution orientation probability.

The variables for each decay will be enumerated as encountered. In general, these variable correspond to the reduced energy of the first two particles listed in the decay.

In the rest frame, these variables emerge naturally as noted above. Usually the mass scale is the $K^0_{\rm L}$ mass, M_K. When using standard Heavyside-Lorentz units ($c = \hbar = 1$), these variables (y and z) are dimensionless, which helps in finding errors in the calculations. It is easy to see how this analysis can be generalized to more than three final state particles. However, there is some difficulty representing a $1 \rightarrow 4$ body Dalitz plot graphically unless some other auxiliary variable is discovered and parameterized. For instance, in a $\mathrm{K}_{l3\gamma}$ decay the auxiliary variable can be written as the angle between the radiated photon and the lepton, and the Dalitz distribution can be shown for several values of the auxiliary variable in a systematic way.

We have used the form factors for the hadronic part of our decays as parametrized in Ref. [2] for our comparisons. Although an update of the Review of Particle Physics[3] was printed this summer (2004), no significant changes to the form factors that were used in our analysis were expected or found.

Decays with hadrons in the final state are calculated in terms of Chiral Perturbation Theory (χPT) if there are at least some leptons in the final state. What is not understood about the hadronic systems is parametrized via form factors which appear both with and without kinematic (energy-momentum) dependence. Details on χPT include [4] and the references therein. An understanding of χPT is not needed to grasp the results presented.

We should note that throughout the document the normalizations of the differential curves is arbitrary and was determined to make the comparison of the matrix elements simple and convenient. Also, on these curves, only the MC output is shown again for convenience.

This note is broken into two parts that cover the additions and amendments to the original KOPIO MC code. First we describe the state of the $K^0_{\rm L}$ decays and the new decay processes that have been added in Section II. Also, we describe the additions to the muon decays in their own right in Section III. Our conclusions are presented in Section IV. Briefly, the decays and their status are listed in Table I and II.

II. $K^0_{\rm L}$ DECAYS

Our $K^0_{\rm L}$ decays can be broken into two categories, semi-leptonic and totally hadronic. The semi-leptonic decays have at least two leptons in the final state, whereas the totally hadronic decays need no real explanation. The semi-leptonic decays are treated in the framework of χPT with measured form factors and the totally hadronic decays are parametrized in terms of Lorentz invariants multiplied by experimentally measured parameters. Therefore, the totally hadronic results have no direct comparison to analytic calculations, but some comments about the distributions are made on statistical grounds.

K_L^0	Final State Particles	Channel	ME	Status
kpnn	$\pi^0\nu\nu$	1	l3	Old
kp2	$\pi^0\pi^0$	2	1	Old
kcp2	$\pi^\pm\pi^\mp$	3	1	Old
kgg	$\gamma\gamma$	4	1	Old
kp3	$\pi^0\pi^0\pi^0$	5	pi3	Old
kcp3	$\pi^\pm\pi^\mp\pi^0$	6	pi3	Rev
ke3	$\pi^\pm e^\mp\nu$	7	l3	Old
km3	$\pi^\pm\mu^\mp\nu$	8	l3	Old
ke3g	$\pi^\pm e^\mp\nu\gamma$	9	kl3g	Old
km3g	$\pi^\pm\mu^\mp\nu\gamma$	10	kl3g	Old
kpgg	$\pi^0\gamma\gamma$	11	pigg	Old
ke4	$\pi^0\pi^\pm e^\mp\nu$	12	l4	Old
km4	$\pi^0\pi^\pm\mu^\mp\nu$	13	l4	Old
ke2g	$e^\pm e^\mp\gamma$	14	1	Bad
km2g	$\mu^\pm\mu^\mp\gamma$	15	1	Bad
kpee	$\pi^0 e^\pm e^\mp$	16	pill	New
kpmm	$\pi^0\mu^\pm\mu^\mp$	17	pill	New

TABLE I: This is a summary of the current state of the MC code. The table shows the nick-name of the process, the actual particles of the decay, the channel number (needed internally for the MC), the name of the matrix elements used for the decay, and if the process was part of the MC when the extensions were added. All of the 'Old' processes except for the K_{l4} decays were checked against analytic calculations. The entry listed as 'Rev' implies that the coefficients were updated for this code, but no significant changes were made. The entries listed as 'Bad' were removed and set to unity due to an error by the author. If the number 1 is in the matrix element column, then a phase space approximation is being used where the matrix elements are set to unity.

$\mu^\pm$	Final State Particles	Channel	ME	Status
	$e^\pm\nu_\mu\bar{\nu}_e$	1	muDecay	New
	$e^\pm\nu_\mu\bar{\nu}_e\gamma$	2	muDecayRad	New
	$e^\pm\nu_\mu\bar{\nu}_e e^\pm e^\mp$	3	1	DNE

TABLE II: All of the muon decays originally used the phase space approximation. The final 5 body decay is not yet implemented (DNE - Does Not Exist) in the MC as of yet. See Section III for more details.

A. Semi-Leptonic Decays

The matrix elements for most of the semi-leptonic K_L^0 decays can be found in Ref. [5] and were shown to be in agreement with those in the PDG[2] (it should be noted, these two references use different normalization schemes for the form factors but [5] gives information on how to compare the two results). A separate derivation for the matrix elements for the signal channel also showed them to be in agreement with the published results. We conclude therefore that the matrix elements in the MC are in agreement with the matrix elements for K_{l3}.

1. $\pi^0 ll$

The signal channel has the same matrix elements as K_{l3} with two massless leptons in the final state. This was an incredible benefit exploited over and over in these calculations and is usually (and correctly) attributed to isospin invariance. There is another way to understand this effect diagrammatically. Because of the nature of χPT, external fermion lines always contribute at tree level only in the form of spinors and a coupling constant. In other words, external leptons have no momentum dependent couplings. This allows the interchange of any external lepton for a different lepton if one takes into account the conservation of charge for the process and the change in coupling. The numeric value for the form factor for each specific process will certainly change (although not its energy dependence due to the universality of the generations), but the analytic portion of the matrix elements will remain the same. This allowed a general derivation for the matrix elements for several processes.

The Dalitz distributions were compared for the following channels, allowing for the appropriate lepton masses and coupling constants. As a side note, the coupling was not of great interest because the matrix elements in the MC code were scaled to lie between zero and unity to be of use to the MC apparatus.

1. $K_{\rm L}^0 \to \pi^0 \nu\bar{\nu}$ ($\Gamma_i/\Gamma < 5.9 \cdot 10^{-7}$)
2. $K_{\rm L}^0 \to \pi^{\pm} e^{\mp} \nu$ ($\Gamma_i/\Gamma = 0.3879$) (K_{e3})
3. $K_{\rm L}^0 \to \pi^{\pm} \mu^{\mp} \nu$ ($\Gamma_i/\Gamma = 0.2718$) ($\mathrm{K}_{\mu 3}$)

A two-dimensional Dalitz distribution was produced by the MC code and from an analytic calculation. The results were projected onto two one-dimensional distributions ($d\Gamma/dy$ and $d\Gamma/dz$). The normalized difference between the theoretical curve and the MC curve was found to be on the order of a few parts in 10^{-3}. Considering the internal storage of the variables in the MC program, it would appear that the two calculations are in perfect agreement. The agreement for these three channels can be seen in Fig. 3.

In Fig. 3 we define the dimensionless variables

$$y = \frac{2E_l}{M_K}, \qquad z = \frac{2E_\pi}{M_K}, \tag{2}$$

where E_l is the energy of the charged lepton (for K_{l3}) which is a good experimental choice as the neutrino will not be observed and for the neutrino in the signal channel. This choice for the signal channel, although not physical, allowed for the matrix elements to be checked in the numeric simulation even though the z spectrum can not be detected. There is another important consideration for decays with identical particles. For instance, we will use similar variables in the $3\pi^0$ decays, but the pions can not be labeled in a realistic way unless they are ordered by their momentum. More on this later.

At the same time, these channels have radiative decays as well that are very important. Here we stress that we are talking about the radiative decays, and not the radiatively corrected decays. The decays are as follows

1. $\pi^{\pm} e^{\mp} \nu\gamma$ ($\Gamma_i/\Gamma = 3.53 \cdot 10^{-3}$) ($\mathrm{K}_{e3\gamma}$)
2. $\pi^{\pm} \mu^{\mp} \nu\gamma$ ($\Gamma_i/\Gamma = 5.7 \cdot 10^{-4}$) ($\mathrm{K}_{\mu 3\gamma}$)

The analysis of these channels is not finished, but the MC code was reviewed and appears to be in agreement with published matrix elements, but not direct comparison is available.

2. $\pi^0\gamma\gamma$ ($\Gamma_i/\Gamma = 1.68 \cdot 10^{-6}$)

This process has no tree-level contributions because there are not enough powers of momentum to satisfy the constraint of gauge invariance[6]. The matrix elements can be broken apart in the usual way

$$\mathcal{M}(K_{\rm L}^0(p) \to \pi^0\gamma(q_1,\epsilon_1)\gamma(q_2,\epsilon_2)) = \epsilon_{1\mu}\epsilon_{2\nu}\mathcal{M}^{\mu\nu}(p,q_1,q_2) \tag{3}$$

The squared matrix elements (here ρ_0) can be written

$$\rho_0(z,y) = \frac{M_K}{(8\pi)^3}\left[z^2(|A+B|^2+|C|^2) + \left(y^2 - \frac{1}{4}\lambda(1,r_\pi^2,z)\right)^2(|B|^2+|D|^2)\right], \tag{4}$$

where $A(z,y)$, $B(z,y)$, $C(z,y)$, and $D(z,y)$ are complex functions, $r_\pi = m_\pi/M_K$ and

$$\lambda(a,b,c) = a^2 + b^2 + c^2 - 2(ab + ac + bc), \tag{5}$$

is the usual 'triangular function', sometimes known as the Källen function. The functions A, B, C are Bose symmetric and D is antisymmetric. These functions parametrize the different possible contributions to the matrix elements in χPT. The y, z variables are uniquely defined as written in these matrix elements for this case (in the rest frame) as

$$y = \frac{2(E_1 - E_2)}{M_K}, \qquad z = \frac{2(E_1 + E_2)}{M_K}, \tag{6}$$

which are superpositions of the usual variables for the two photons. The results found in Fig. 4 use the usual definition of the y, z variables with $y = 2E_\pi/M_K$ and $z = 2E_1/M_K$.

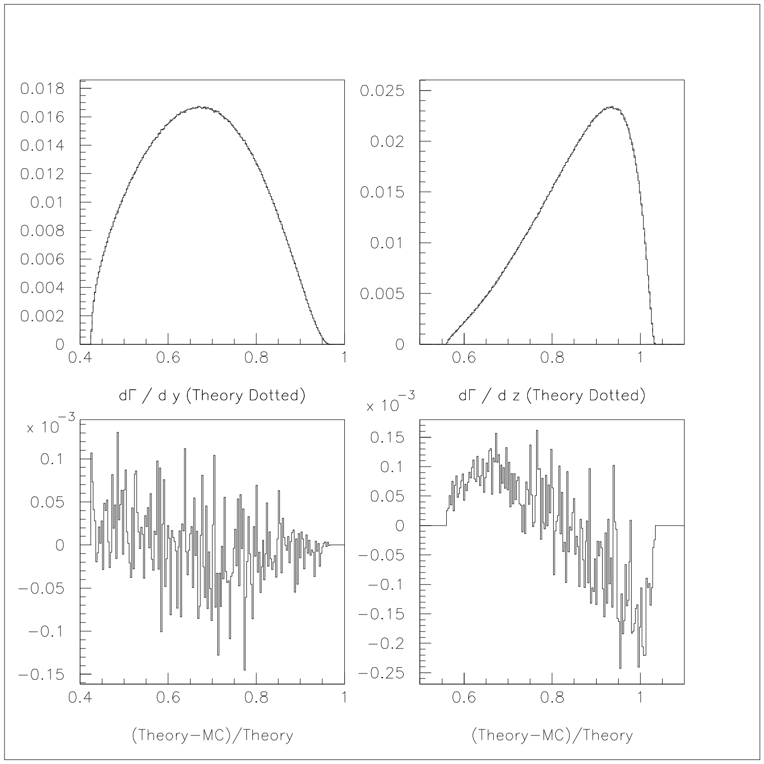

(a)

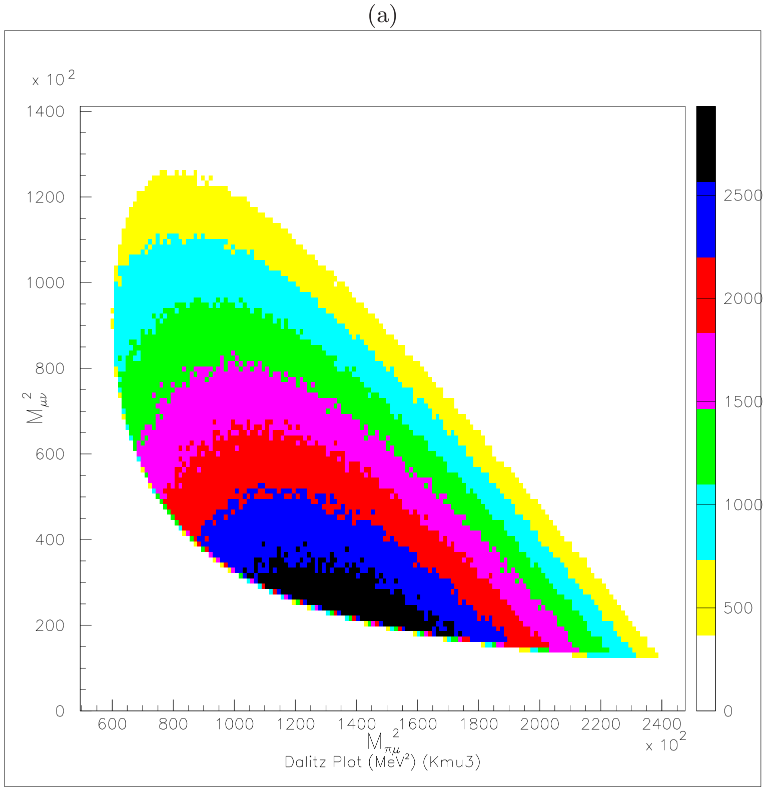

(b)

FIG. 3: A comparison of the MC and an analytic calculation of the matrix elements for $K_{\mu 3}$. The agreement is representative of the agreement with the signal channel and K_{e3} as they have the same matrix elements. Here, as in the rest of this note, the units of the distributions are arbitrary. The Dalitz plot shown in Figure 3b shows that the preferred decay orientation is for the pion to come out opposite the two leptons. The variables in Figure 3a are defined as $y = 2E_l/M_K$ and $z = 2E_\pi/M_K$.

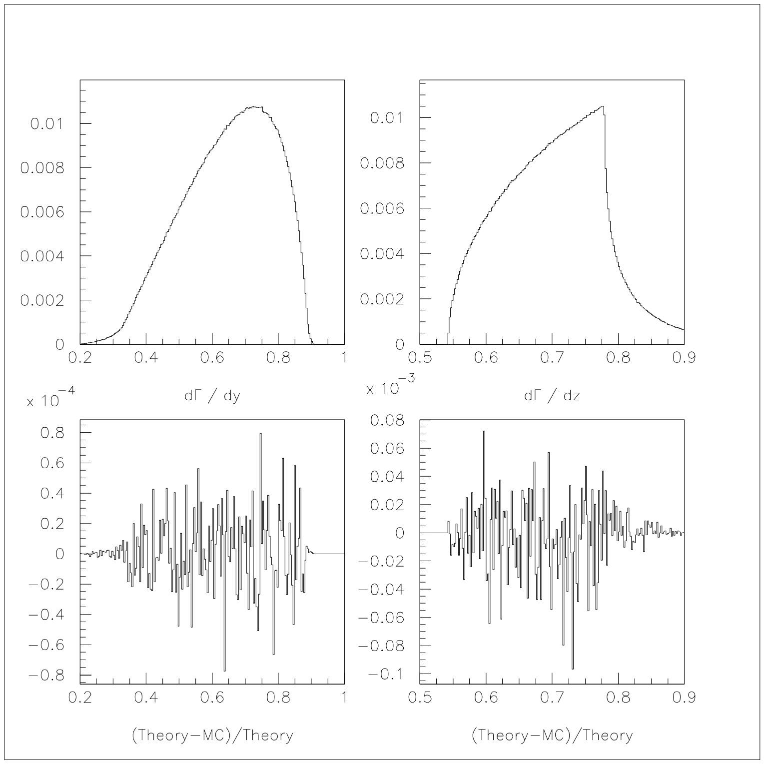

(a)

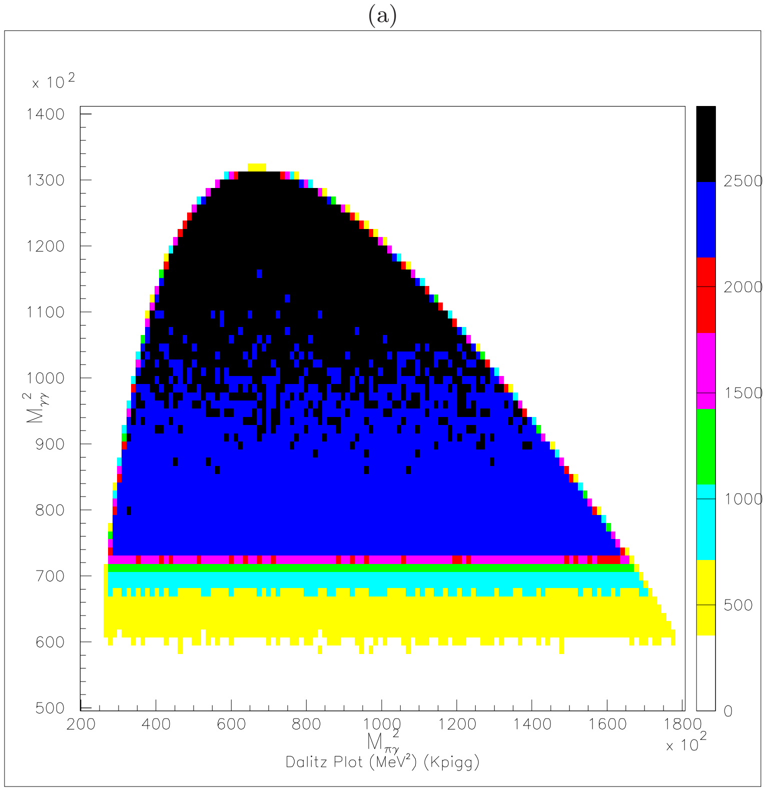

(b)

FIG. 4: Figure 4a shows $\pi^0\gamma\gamma$ and Figure 4b shows the Dalitz plot. Although it is not particularly clear in this case, the Dalitz plot continues all the way to the bottom of the graph, but at very small levels. We can see in this analysis that the preferred decay orientation is for the two photons to leave in opposite directions leaving the π^0 at rest. The variables in Figure 4a are defined as $y = 2E_\pi/M_K$ and $z = 2E_1/M_K$.

3. $\pi^0\pi^\pm l^\pm\nu$

These decays are complicated in that they are computationally difficult. The matrix elements are parametrized by four real analytic function of three variables as form factors. The total decay width (the integrated Dalitz distribution) has to be expressed in terms of scalar products of five independent variables and a seven dimensional integral. Fortunately, we are interested in the matrix elements and the Dalitz distribution, and not the total width. The four body decays are

1. $\pi^0\pi^\pm e^\mp\nu$ ($\Gamma_i/\Gamma = 5.18 \cdot 10^{-5}$) ($\mathrm{K}_{e4}$)
2. $\pi^0\pi^\pm \mu^\mp\nu$ ($\Gamma_i/\Gamma = 6.42 \cdot 10^{-6}$) ($\mathrm{K}_{\mu4}$)

where is should be noted that the $\mathrm{K}_{\mu4}$ decay rate appears in only one place in the literature[7] (this is a theoretical paper, the decay have not been measured) and the calculation is somewhat dated so the quoted branching ratio should be taken with a gain of salt. Because of time constraints, these decays were not studied in detail. The code in the MC was examined and appeared to be in agreement with the literature, but no detailed comparisons are available.

4. $\pi^0 l^\pm l^\mp$

Next, we considered the following decays.

1. $\pi^0 e^\pm e^\mp$ ($\Gamma_i/\Gamma < 5.1 \cdot 10^{-10}$) [**New**]
2. $\pi^0 \mu^\pm \mu^\mp$ ($\Gamma_i/\Gamma < 3.8 \cdot 10^{-10}$) [**New**]

These decays are interesting in that they have a CP-violating piece that is like the signal channel. In general, the decay amplitude has three possible contributions: 1) a direct CP-violating piece from electroweak and W-box penguin diagrams, 2) an indirect CP-violating piece, and 3) a CP-conserving piece from the $\pi^0\gamma\gamma$ intermediate state. A detailed analysis is available in Ref. [8, 9]. We used the same assumptions about the magnitude of the three terms as in Ref. [9].

Generically, the matrix elements are parametrized in χPT in terms of a scalar, vector, pseudoscalar, and axial-vector components. Following Ref. [9], we can write the matrix elements (written here as ρ_0) as follows

$$\Gamma = \frac{m^2}{2M_K}\int \rho_0(E,\bar{E})\frac{dE\,d\bar{E}}{(2\pi)^3} \tag{7}$$

Here, we have chosen to simplify the notation somewhat. To be exact, let is consider the reaction $K_{\mathrm{L}}^0 \to \pi^0 l\bar{l}$ (and let $m_l = m$) so that our variables are obvious, $E = E_l$ and $\bar{E} = E_{\bar{l}}$. If we let $s = (p_l + p_{\bar{l}})^2$ we find

$$\begin{aligned} m^2\rho_0(E,\bar{E}) = {} & |F_S|^2\frac{(s-4m^2)}{2} + |F_P|^2\frac{s}{2} + |F_V|^2 M_K^2(2E\bar{E} - \frac{s}{2}) \\ & + |F_A|^2 M_K^2(2E\bar{E} - \frac{s-4m^2}{2}) + 2\mathrm{Re}(F_S F_V^\star) m M_K(\bar{E} - E) \\ & + 2\mathrm{Re}(F_P F_A^\star)\frac{m}{2}(M_K^2 - M_\pi^2 + s). \end{aligned} \tag{8}$$

The subscripts on the form factors indicate the nature of the contribution (scalar, pseudoscalar, et cetera). The form factors are complicated and have energy dependence and involve complex arithmetic (with imaginary parts) from the contribution from the penguin loop diagrams. The complete expressions are rather lengthy to include here, but can readily be found in the literature listed above.

The dimensionless variables used in this analysis are

$$y = \frac{2E}{M_K}, \qquad z = \frac{2\bar{E}}{M_K}. \tag{9}$$

These decays appear in the Dalitz plots shown in Fig. 5 and Fig. 6. In the $\pi^0 e^\pm e^\mp$ case, we see a preference to have the pion come out opposite nearly colinear electrons in two different configurations. The mass effects in the $\pi^0\mu^\pm\mu^\mp$ case are more pronounced, as the masses of the muon and pion are on the same order. We see a similar configuration to the distributions shown in Ref. [9].

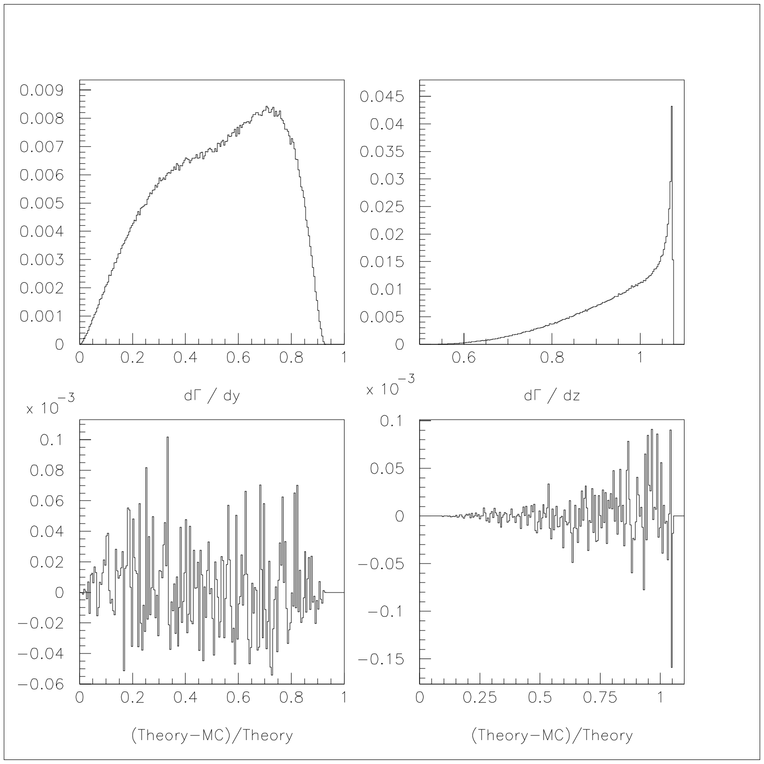

(a)

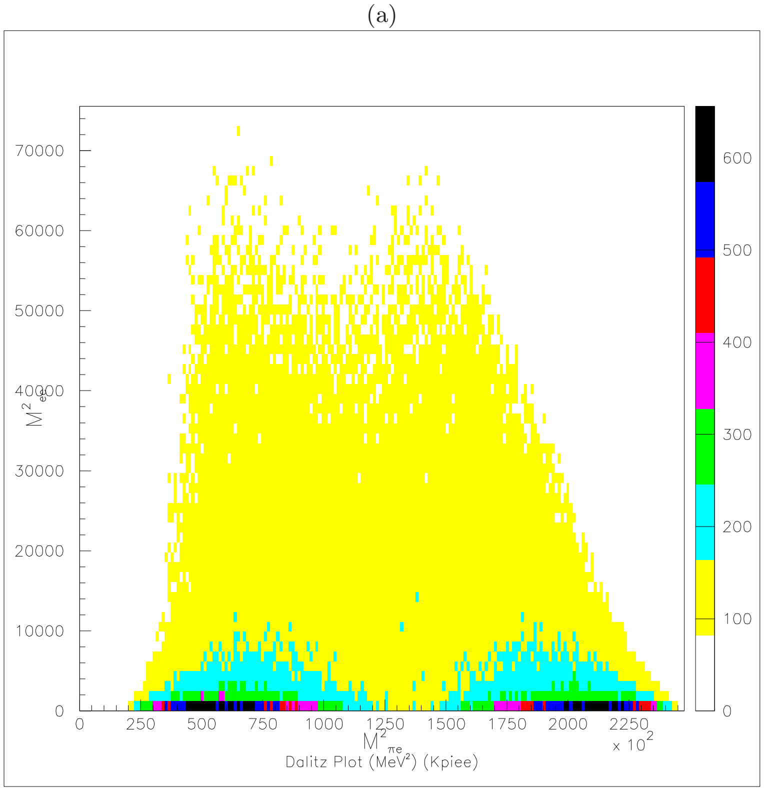

(b)

FIG. 5: Figure 5a shows $\pi^0 e^{\pm} e^{\mp}$ and Figure 5b shows the Dalitz plot. We see that the trend is to have the pion recoil against nearly colinear electrons in both possible configurations. The bimodal nature of the distribution can be attributed to the fact that the electrons are fermions. The variables in Figure 5a are defined as $y = 2E_\pi/M_K$ and $z = 2E_e/M_K$.

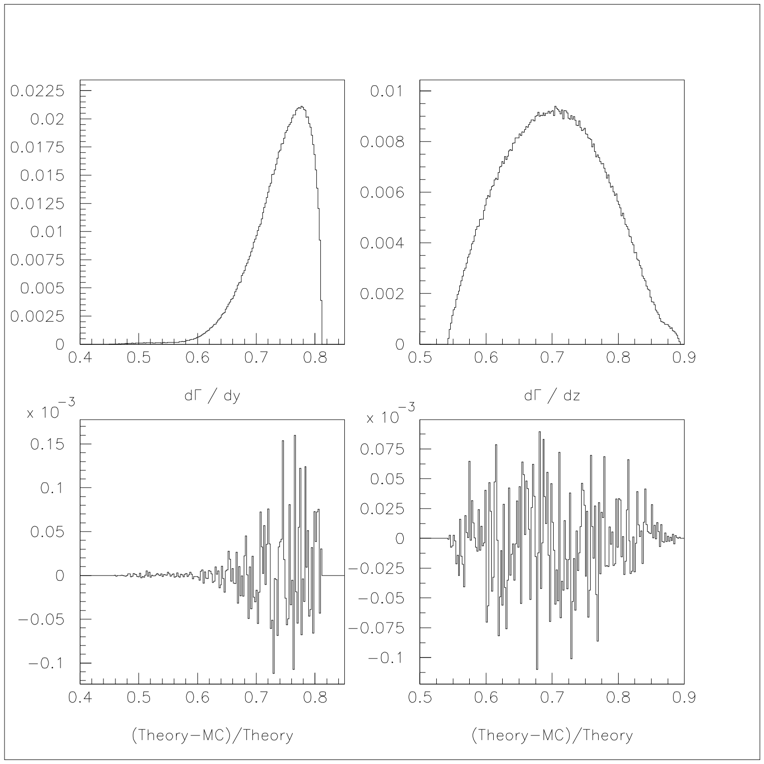

(a)

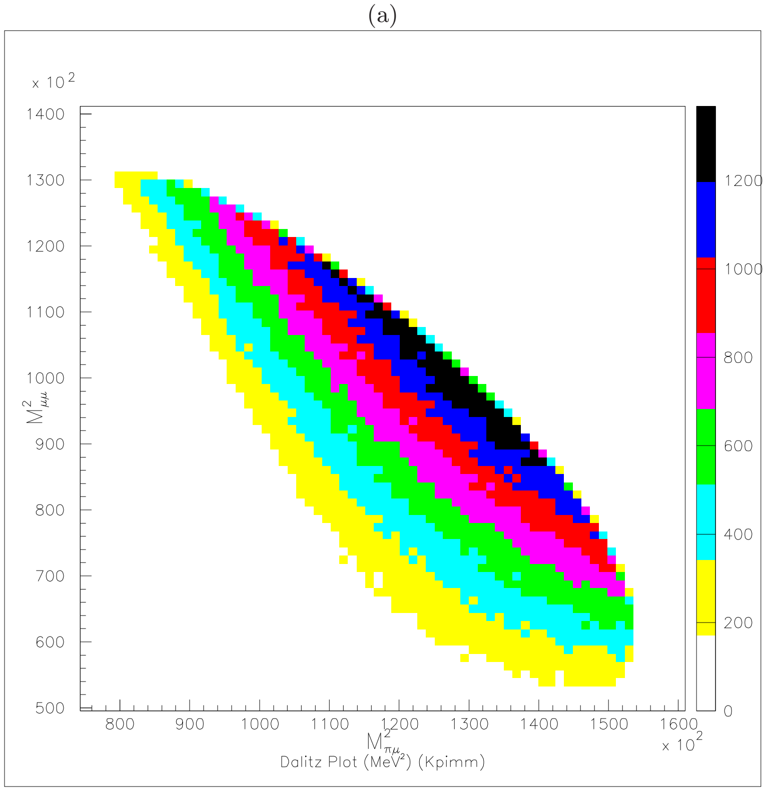

(b)

FIG. 6: Figure 6a shows $\pi^0\mu^\pm\mu^\mp$ and Figure 6b shows the Dalitz plot. The "kidney bean" shape is due to the similarity in the masses of the final products. The variables in Figure 6a are defined as $y = 2E_\pi/M_K$ and $z = 2E_\mu/M_K$.

5. $l^{\pm}l^{\mp}\gamma$

1. $\nu\bar{\nu}\gamma$ ($\Gamma_i/\Gamma = 2\cdot 10^{-13}$) **[New]**
2. $e^{\pm}e^{\mp}\gamma$ ($\Gamma_i/\Gamma = 10.0\cdot 10^{-6}$) **[New]**
3. $\mu^{\pm}\mu^{\mp}\gamma$ ($\Gamma_i/\Gamma = 3.59\cdot 10^{-7}$) **[New]**

It was shown in Ref. [10] that when the first decay in the section ($\gamma\nu\bar{\nu}$) is considered as a loop diagram, it is larger than the tree level decay with a virtual Z^0 boson which had an expected (and essentially unmeasurable) branching ratio $\Gamma_i/\Gamma \approx 10^{-18}$. It would not be hard to argue that this is the least studied background process to the signal channel as it is not even listed as a standard decay by the PDG.

The dimensionless variables used in this analysis are

$$y = \frac{2E_{l+}}{M_K}, \qquad y = \frac{2E_{l-}}{M_K}. \tag{10}$$

in the case of the decays with two charged leptons, and is the energy spectrum of the neutrinos in the case of the $\nu\bar{\nu}\gamma$ decay. Although the reader may be wondering if the comments about a non-physical observable are being taken seriously, we remind ourselves that these variables were used to check the dynamics only and are not to be confused with physical observables of any kind. In the case of $\nu\bar{\nu}\gamma$ the Dalitz plot is triangular because it has three massless particles in the final state. This state is not currently implimented in the MC, but can be with the use of the matrix elements that have been included already.

Since this is formally a loop diagram, the matrix elements have imaginary parts that cancel in the modulus squared. Formally, one should also ask about the inclusion of this process in the MC code because it occurs at a different order than the other processes, but the resolution of this problem is easy to see. Since we have included $1 \to 4$ and $1 \to 5$ body decays, we can include a one-loop $1 \to 3$ decays without worrying about mismatching the order of the calculation or having to add the loop corrections to our other processes, a rather large task.

The $e^{\pm}e^{\mp}\gamma$ and $\mu^{\pm}\mu^{\mp}\gamma$ decays were set back to unity matrix elements due to a physics error on the part of the author.

B. Hadronic Decays

As opposed to the semi-leptonic $K^0_{\rm L}$ decays, the totally hadronic decays cannot be calculated from first principles, even in the context of χPT. Although some studies of these decays have been made on the lattice (which has its own rich literature), the results are not relevant for our purposes. Moreover, most of the lattice results are formulated in the quenched approximation where dynamic fermions are not implemented. In the end, the totally hadronic matrix elements are parametrized in terms of Lorentz invariant quantities with unknown coefficients which are measured by experiments. These decays have no theoretical curves, but some information can be learned from the Dalitz distributions.

This is the appropriate place for some more comments in the ability to distinguish between final state particles. All our comments on whether an spectrum is observable or not still hold, with a few additional conditions. The variables used here are

$$y = \frac{2E_{\pi^0_1}}{M_K}, \quad z = \frac{2E_{\pi^0_2}}{M_K}, \qquad \text{and} \qquad y = \frac{2E_{\pi^+}}{M_K}, \quad z = \frac{2E_{\pi^-}}{M_K}, \tag{11}$$

for the $3\pi^0$ and $\pi^0\pi^{\pm}\pi^{\mp}$ cases respectively listed below.

Now, these are identical particles and it is not possible to actually separate these particles in a detector as it is possible in the matrix elements in the MC. However it would be possible to separate these variables into high and low energy variables, but this was not attempted in our analysis.

1. $\pi^0\pi^0\pi^0$ ($\Gamma_i/\Gamma = 0.2108$)

As expected from Bose symmetry, the $3\pi^0$ decay is symmetric with respect to the three π^0's. The surface of the Dalitz distribution is flat on top, telling is that there is no preferred decay orientation as expected. This is shown in Fig. 7.

2. $\pi^{\pm}\pi^{\mp}\pi^{0}$ ($\Gamma_i/\Gamma = 0.1258$)

Although the $\pi^0\pi^{\pm}\pi^{\mp}$ decay is also Bose symmetric, the two charged pions change the distribution slightly. The preferred decay orientation has the two charged pions leaving back to back with the neutral π^0 left at rest. This is shown in Fig. 8.

C. Other Decays

After inspecting the included decays and some other possible decays may need to be included in the MC code. The following K_{L}^0 decays should be examined by the group to see if they should be included.

1. $\pi^{\pm}\pi^{\mp}\gamma$
2. $\pi^0 l^{\pm} l^{\mp}\gamma$
3. $l^{\pm}l^{\mp}\gamma\gamma$

III. MUON DECAYS

There will be a copious amount of muons produced in the KOPIO experiment. The exact decay properties of muons are understood very well so implementing the decays exactly makes sense.

The muon decays are fundamentally different from the hadronic and semi-leptonic K_{L}^0 decays in that they are exactly calculable in QFT. Although muons have an overwhelming branching ratio into one particular decay channel, the sheer number of muons produced in the experiment require an exact handling of all three of the known decay channels. Currently, the first two of them are implemented.

A. $\mu^{\pm} \to e^{\pm}\nu\bar{\nu}$ ($\Gamma_i/\Gamma = 0.986$) [New]

This is a very well studied decay, the standard bearer of modern particle physics. Originally, this decay was encoded in the MC with matrix elements equal to unity. This was a phase space approximation, that was corrected with the implementation of the exact matrix elements. The decay results can be seen in Fig. 9.

B. $\mu^{\pm} \to e^{\pm}\nu\bar{\nu}\gamma$ ($\Gamma_i/\Gamma = 0.014$) [New]

This decays is the background to $\mu^{\pm} \to e^{\pm}\gamma$ process, and has therefore been well studied[11]. This is the standard radiative decay.

C. $\mu^{\pm} \to e^{\pm}\nu\bar{\nu}e^{\pm}e^{\mp}$ ($\Gamma_i/\Gamma = 3.4 \cdot 10^{-5}$) [New]

This is a radiative decay with an off-shell photon (or Z^0 boson) that decays into an $e^{\pm}e^{\mp}$ pair. This is perhaps the most complicated decay that has been considered in this note, even though it is exactly solvable. This is from the sheer number of variables and mass scales. In the full version of this decay, virtual $W^{\pm}$ and Z^0 bosons appear which have complicated couplings. The matrix elements for this decays are not currently available to the MC code. As a note to whomever may continue this work, the matrix elements may be simplified considerable if the Z^0 contributions and the contributions with WWZ couplings are ignored. Since the $\mu^{\pm}$ decays via a virtual $W^{\pm}$ boson and the muons created will not be incredibly energetic and it would seem unlikely that two virtual particle would be created in the decay process and these vertices and contributions can be safely ignored as a first approximation.

IV. RESULTS AND CONCLUSIONS

Overall, the KOPIO MC appears to be in excellent agreement with the theoretical analysis with most of the differences being accounted for in round-off errors in the internal representation of the variables.

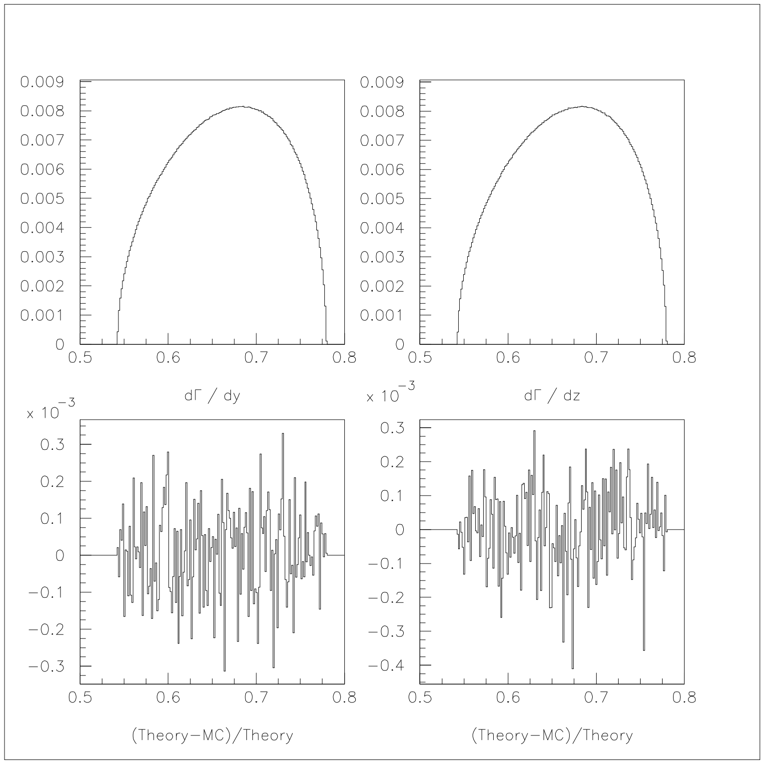

(a)

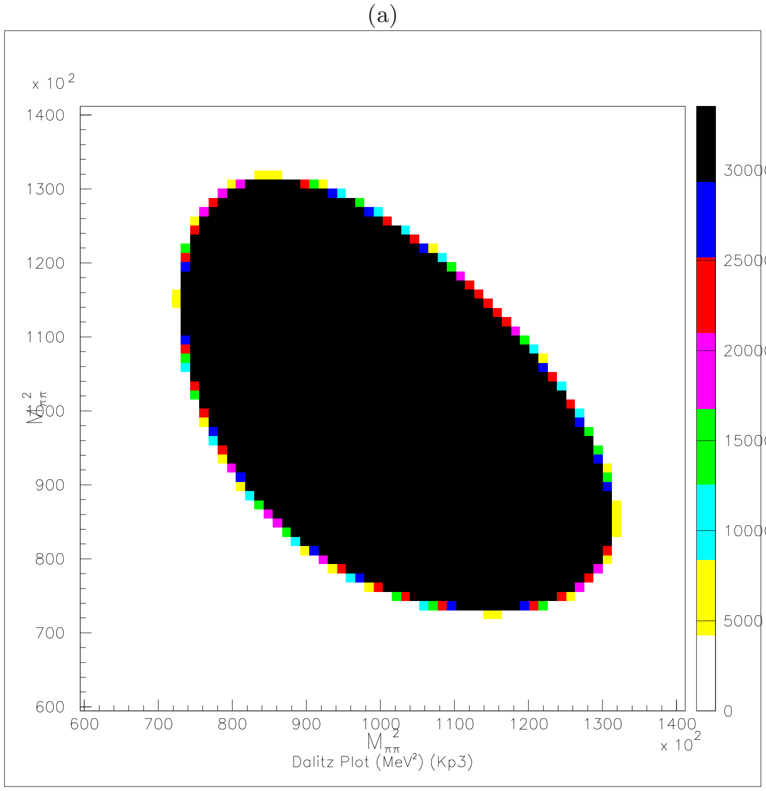

(b)

FIG. 7: Figure 7a shows $3\pi^0$ and Figure 7b shows the Dalitz plot. We can see that the Dalitz plot is uniformly populated as expected from the Bose statistics. This shows no particular decay orientation is preferred for this channel. The variables in Figure 7a are defined as $y = 2E_{\pi_1^0}/M_K$ and $z = 2E_{\pi_2^0}/M_K$.

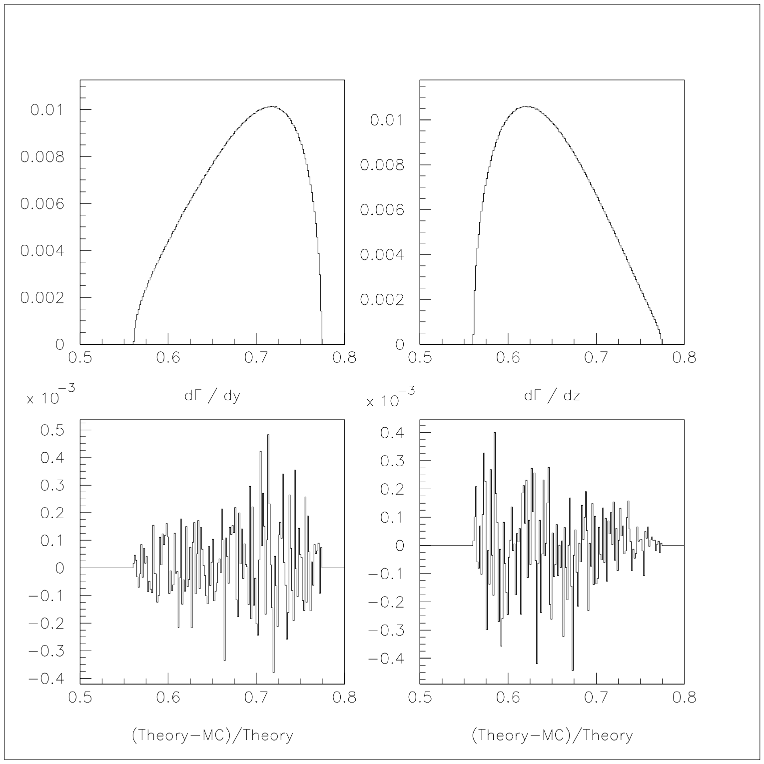

(a)

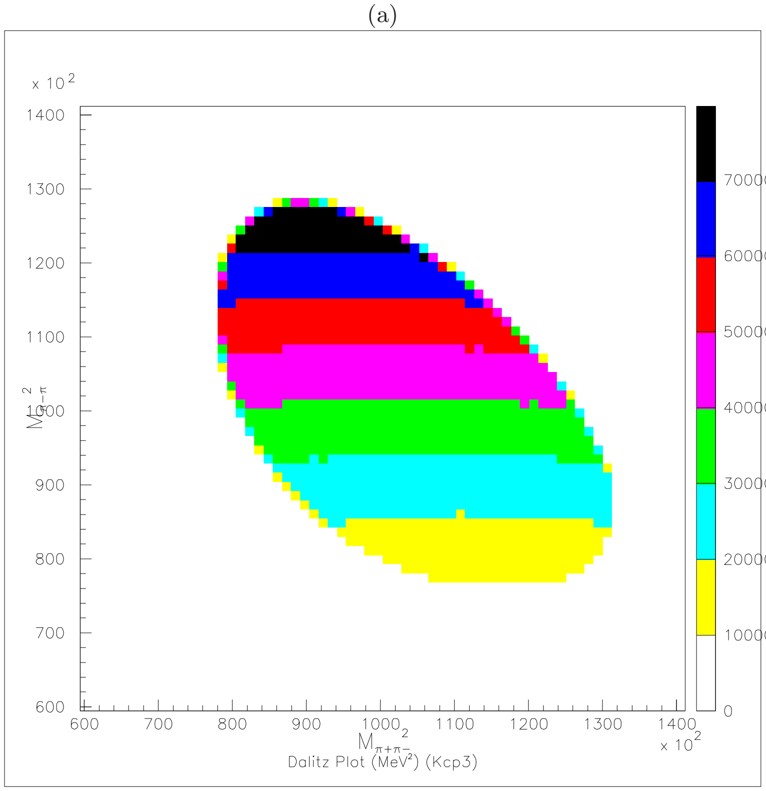

(b)

FIG. 8: Figure 8a shows $\pi^0\pi^\pm\pi^\mp$ and Figure 8b shows the Dalitz plot. We can see that the Dalitz plot is not completely uniform. Although the Bose statistic argument holds, the charge of the final state pions is coming into play here. The preferred decay orientation have the neutral π^0 stationary and the two charged $\pi^\pm$ leaving back to back. The variables in Figure 8a are defined as $y = 2E_{\pi^+}/M_K$ and $z = 2E_{\pi^-}/M_K$.

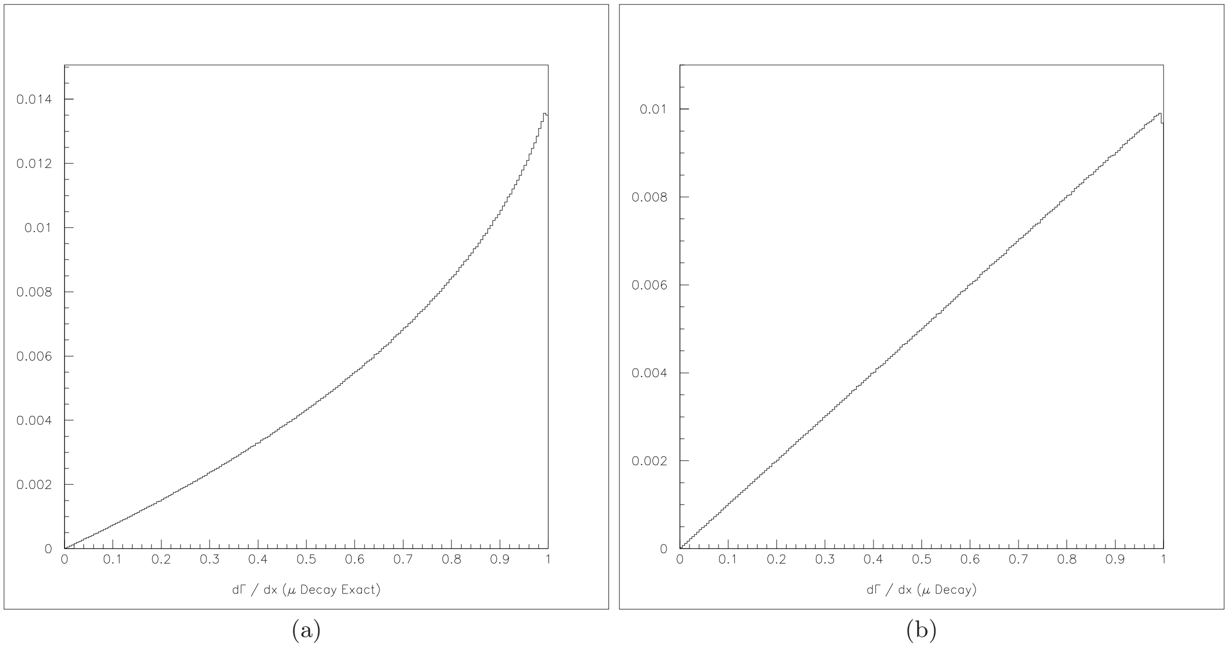

FIG. 9: The standard $\mu^{\pm} \rightarrow e^{\pm}\nu\bar{\nu}$ decay. Figure 9a show the exact reduced energy spectrum of the electron whereas Figure 9b is the same spectrum in the phase space approximation. It is easy to see that the exact expression yielded improvement over the approximation. The primary difference in the curves comes from the mass effects included in the matrix elements. In these figures we have define $x = 2E_e/M_\mu$.

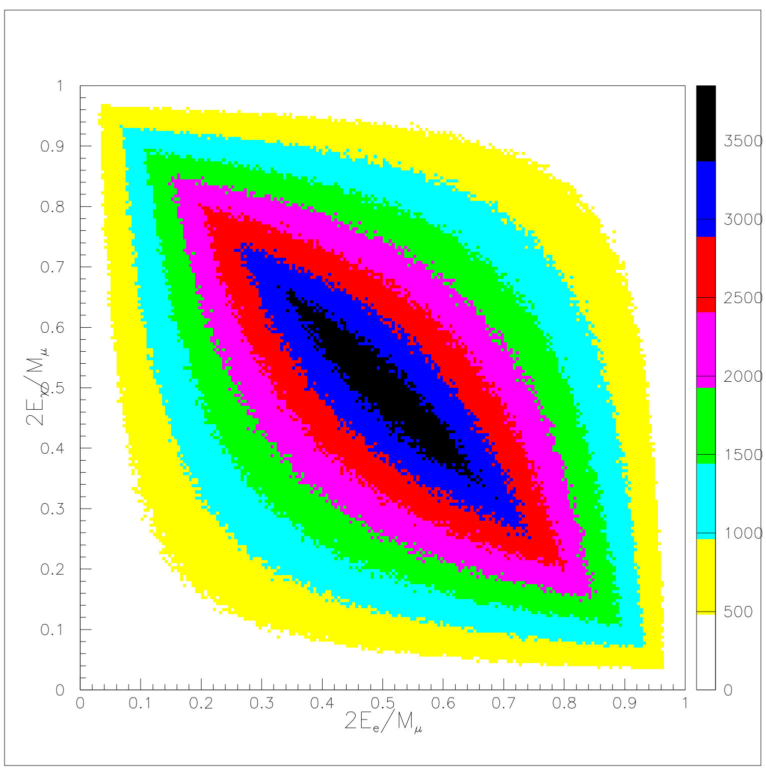

FIG. 10: This shows the energy spectrum of the electron and the photon for the radiative muon decay. This cannot directly be compared to the other decays because this is a $1 \rightarrow 4$ body decay.

Acknowledgments

The author would like to thank the KOPIO group, in particular David Jaffe and Michael Marx for their hospitality and support during the summer.

---

[1] E. Byckling and K. Kajantie, "*Particle Kinematics*," John Wiley and Sons, 1973.
[2] K. Hagiwara *et al.* [Particle Data Group Collaboration], Phys. Rev. D **66**, 010001 (2002).
[3] S. Eidelman *et al.* [Particle Data Group Collaboration], Phys. Lett. B **592**, 1 (2004).
[4] S. Scherer, arXiv:hep-ph/0210398.
[5] J. Bijnens, G. Colangelo, G. Ecker and J. Gasser, arXiv:hep-ph/9411311.
[6] G. D'Ambrosio and J. Portoles, Nucl. Phys. B **492**, 417 (1997) [arXiv:hep-ph/9610244].
[7] T. Becherrawy and N. F. Nasrallah, Phys. Rev. D **14**, 1799 (1976).
[8] J. F. Donoghue and F. Gabbiani, Phys. Rev. D **51**, 2187 (1995) [arXiv:hep-ph/9408390].
[9] M. V. Diwan, H. Ma and T. L. Trueman, Phys. Rev. D **65**, 054020 (2002) [arXiv:hep-ph/0112350].
[10] W. J. Marciano and Z. Parsa, Phys. Rev. D **53**, 1 (1996).
[11] Y. Kuno and Y. Okada, Rev. Mod. Phys. **73**, 151 (2001) [arXiv:hep-ph/9909265].